Cycle 47R1 overview

Andy Brown

Director of Research

ECMWF

Data assimilation and Observation highlights

- Revised weak-constraint 4D-Var
- Situation-dependent skin temperature background error variances from EDA
- Shorter timestep in last 4D-Var minimisation
- First guess in delayed cutoff 12-hour 4D-Var obtained from early delivery
- Revised ATMS observation errors
- Channel specific aerosol rejections for IR sounders
- Spline interpolation in the 2D GPS-RO bending angle operator

Weak-constraint 4D-Var

Strong constraint 4D-Var

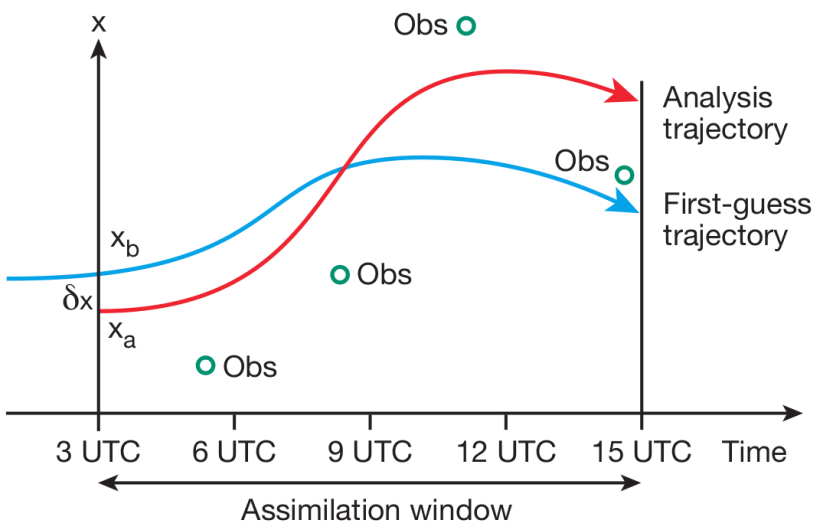

Weak constraint 4D-Var

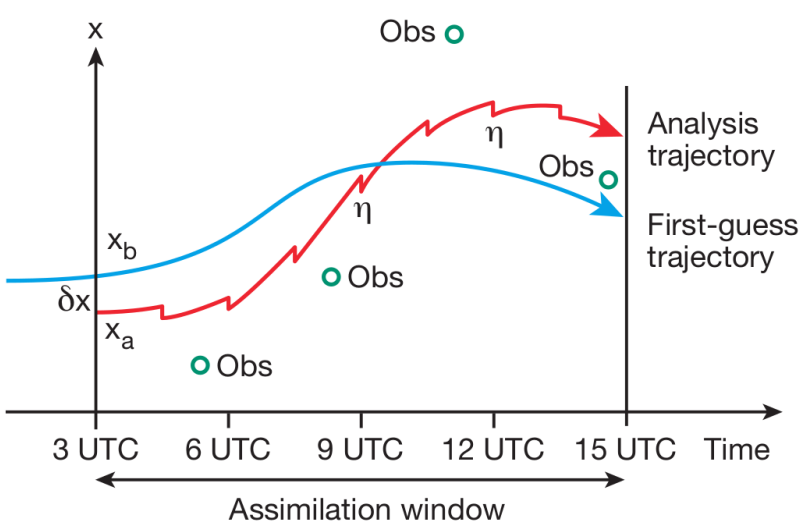

Weak-constraint 4D-Var

- A new estimate of the model error covariance matrix has been computed from a climatology of the model error vectors estimated by the current weak-constraint 4D-Var [Laloyaux et al., 2020b].
- Now the length scales that weak-constraint 4D-Var targets are much longer than those corrected by the B component of 4D-Var (and similar to the length scales of the patterns in the figure opposite).

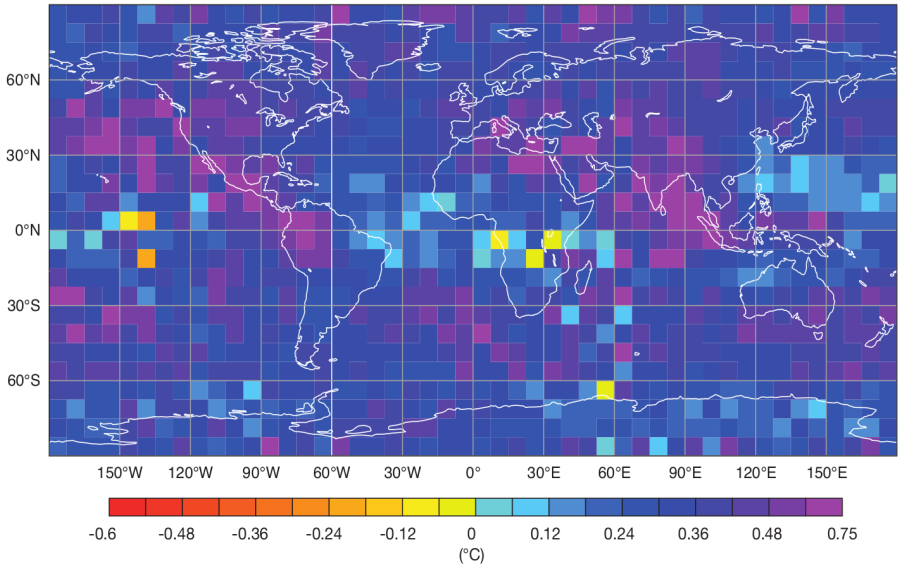

Difference between radio occultation temperature retrievals and first-guess temperatures from ECMWF operations between 70 hPa and 100 hPa over the period 31 August 2018 to 31 January 2019.

Weak-constraint 4D-Var

- The weak-constraint 4D-Var currently used in operations corrects only a small fraction of the model bias over 40 hPa, while the new model error covariance matrix better corrects the diagnosed cold and warm biases of the model over 100 hPa, reducing the mean error by up to 50%.
- The results show that bias in the upper stratosphere located between 30 km and 45 km (11 hPa to 1.5 hPa) is also significantly reduced in the new system

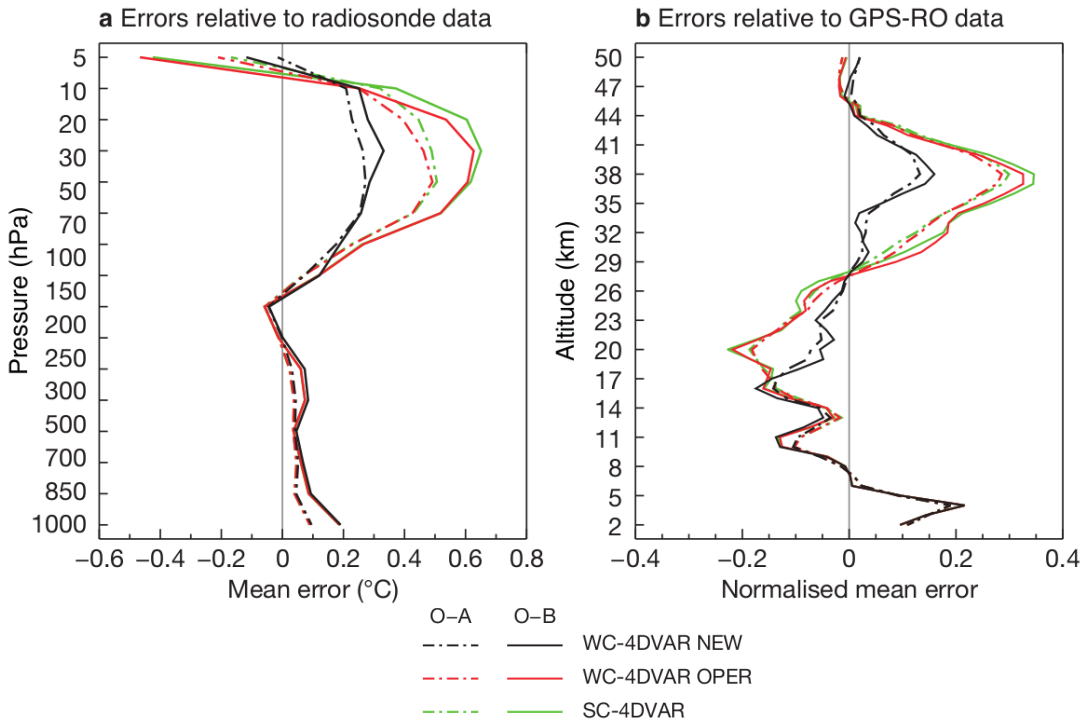

Vertical profiles of mean analysis (O–A) and background departures (O–B) with respect to (a) radiosonde observations and (b) radio occultation observations (GPS-RO). The statistics were computed for the period from 1 October 2018 to 1 April 2019

Skin temperature background errors

- The magnitude of the skin temperature adjustment is controlled by a background error term, defined at the observation locations and in CY46R1 set to 5K over land.
- New spatially and time varying background errors for skin temperature have been derived based upon output from the Ensemble of Data Assimilations (EDA).
- Hence observations from LEO satellites now have flow dependent background errors which control the adjustment of the surface by the satellite.

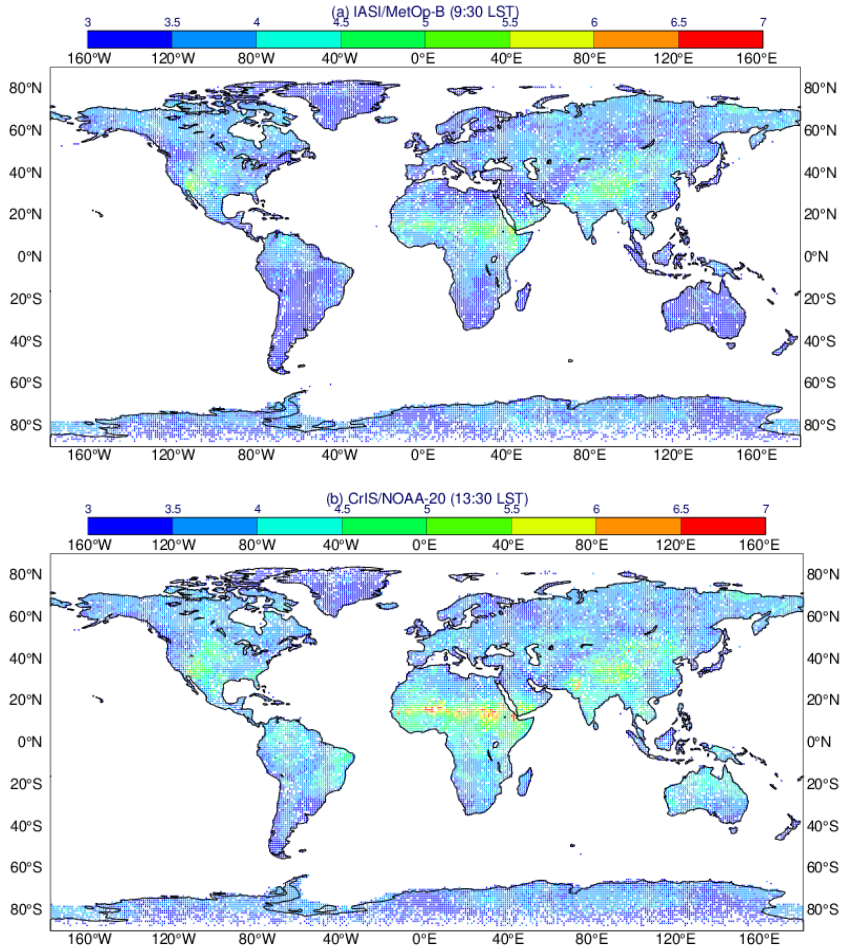

Shorter timestep in final 4D-Var minimisation

- In CY46R1 the inner loop minimisation timestep is double that used in the outer loops (900s vs 450s)
- This introduces a significant difference in the propagation speed of gravity waves in outer versus inner loop integrations, with the result that spurious gravity-wave-like increments are generated during the 4D-Var analysis
- Running only the last minimisation with the same time step in both inner and outer loop is sufficient to suppress the spurious gravity waves in the increments and analysis.

Temperature increments at ~100hPa

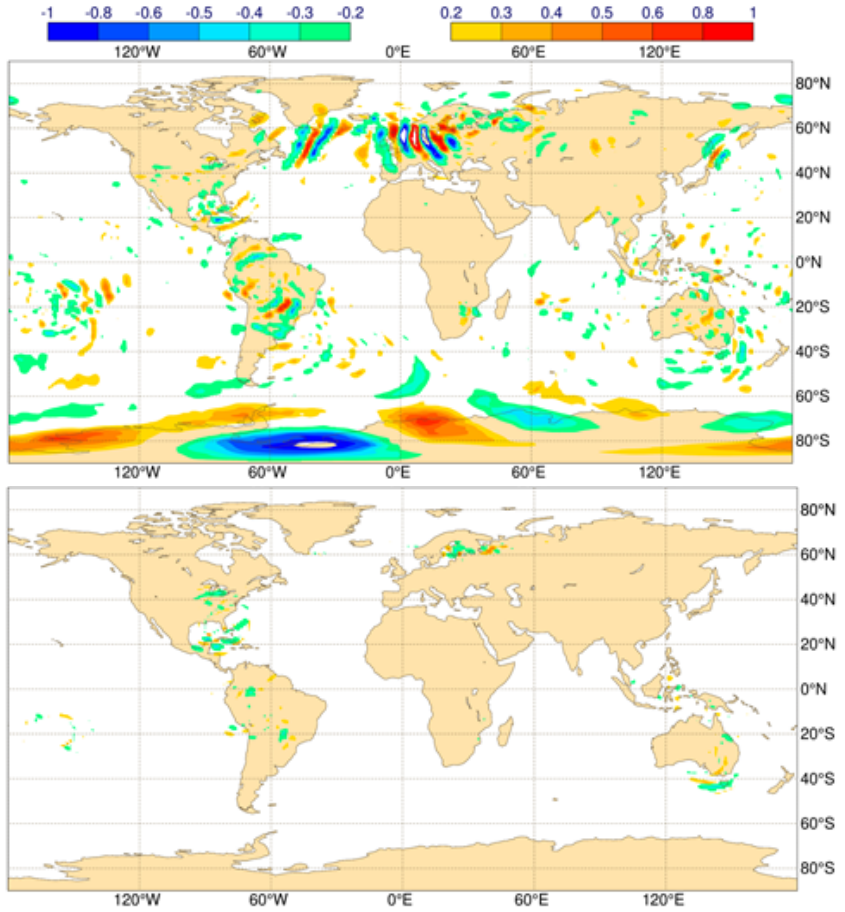

Shorter timestep in final 4D-Var minimisation

- 6% increase in the computational cost of the analysis
- Clear improvements to stratospheric analyses and forecasts, and a smaller but statistically significant impact on tropospheric skill
- Monotonic convergence of incremental 4D-Var in atmospheric situations where current incremental 4D-Var can struggle to converge (e.g., Sudden Stratospheric Warming events)
- Considerable improvement of initial balance of the 4D-Var analysis

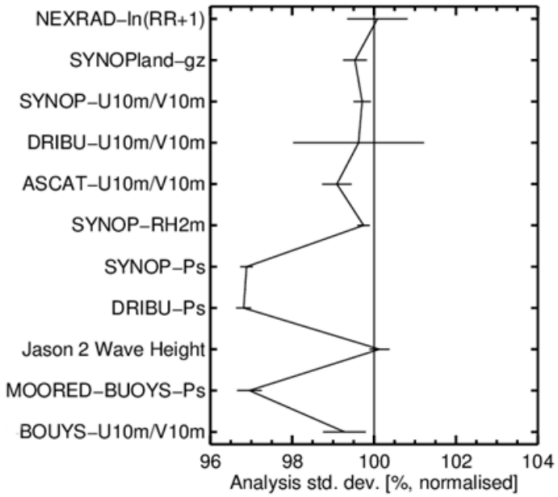

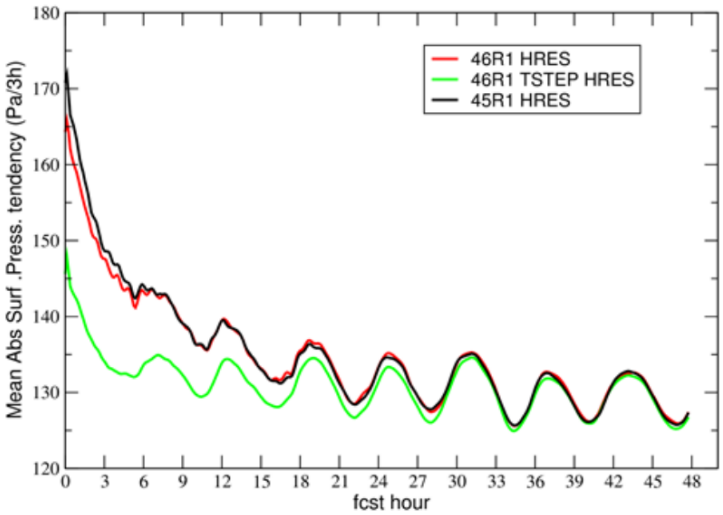

First guess from Early Delivery

- Warm start LWDA from previous ED analysis :
  - LWDA (12h)/ED (8h) use same background x_b .
  - First guess LWDA differs: $x_{fg}^{LW} = x_b^{LW} + B^{1/2}\chi^{ED}$.
- Equivalent to increasing the number of outer loops at no additional computational cost.
- Significant positive impact on nonlinear observations (humidity/cloud/precipitation).

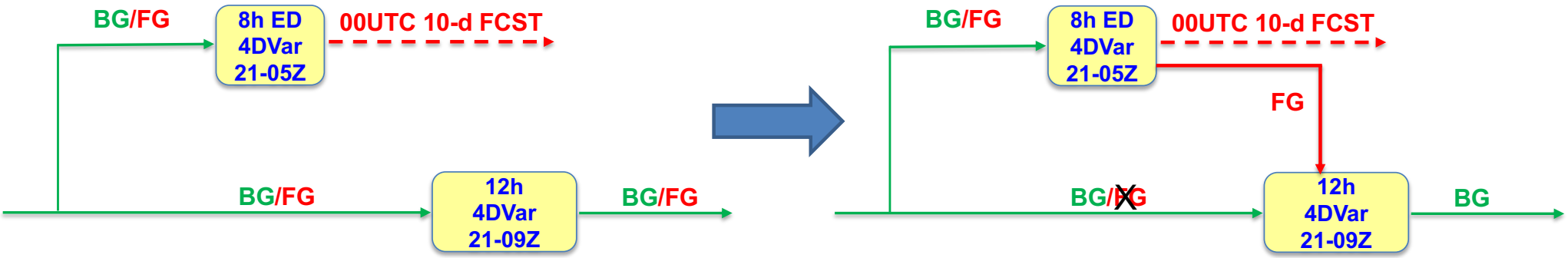

Continuous Long-window data assimilation

- This contribution reduces background observation departures
- Increased RMSE in own analysis verification - not seen in verification against an independent analysis like ERA5 or against observations

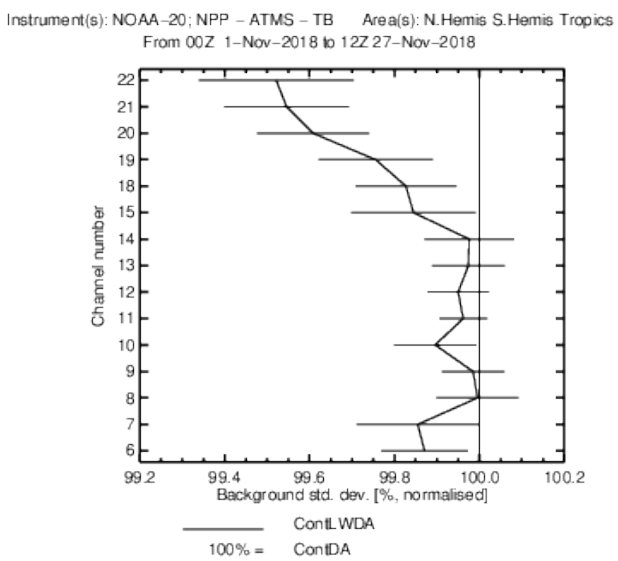

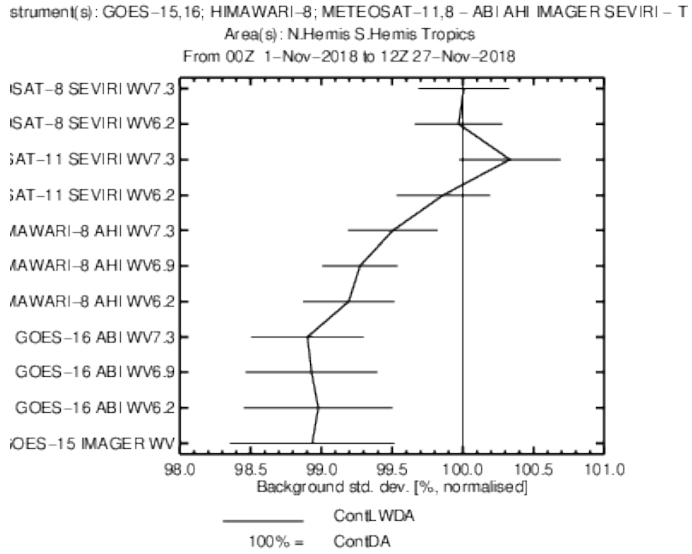

Model highlights

- Quintic vertical interpolation in semi-Lagrangian advection
- Modified Charnock parameter for high windspeeds occurring in tropical cyclones
- Surface albedo changes
- Update to greenhouse gases and total solar irradiance
- Updates to the convection scheme
- Improvements to the tangent-linear physics

Quintic vertical interpolation in semi-Lagrangian advection

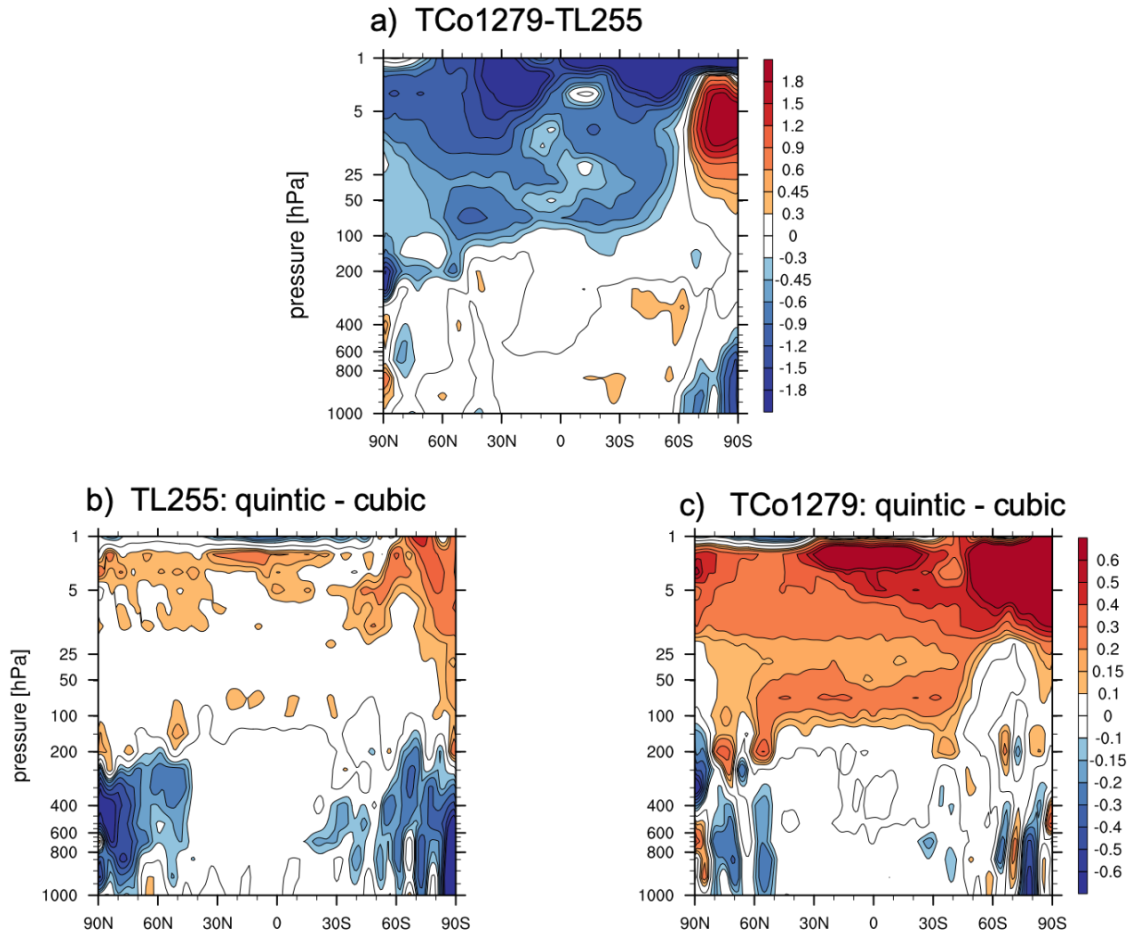

- Undesirable resolution sensitivity due to insufficient vertical resolution
- Spurious global-mean cooling in the stratosphere at high horizontal resolution in IFS
- Increasing vertical resolution in stratosphere is expensive
- Quintic vertical interpolation of advected fields evaluated at the departure point alleviates the problem
- Quintic interpolation replaces cubic interpolation for T and q

Relative change in temperature RMSE in HRES

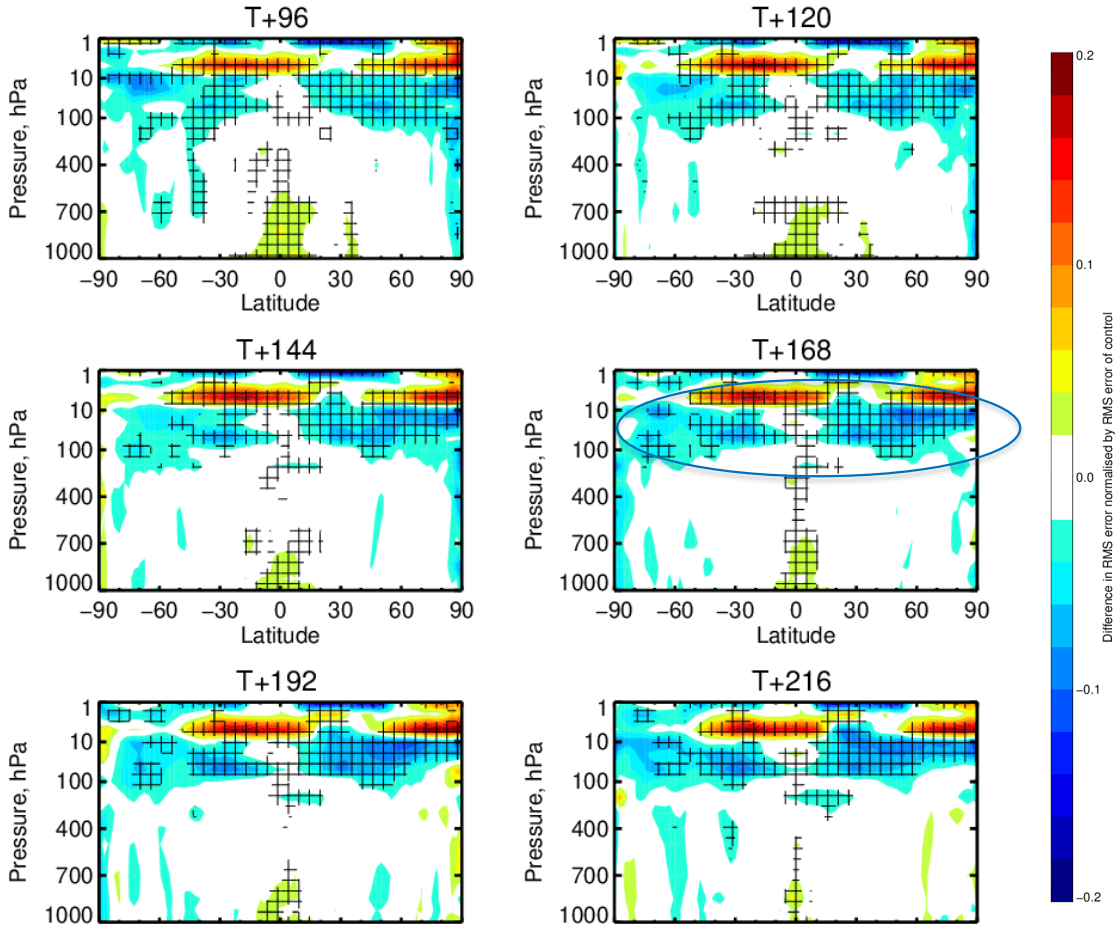

- Improves lower stratosphere scores significantly
- Upper stratosphere degrades due to pre-existing warm bias of the model

Revision of drag as function of wind speed over ocean

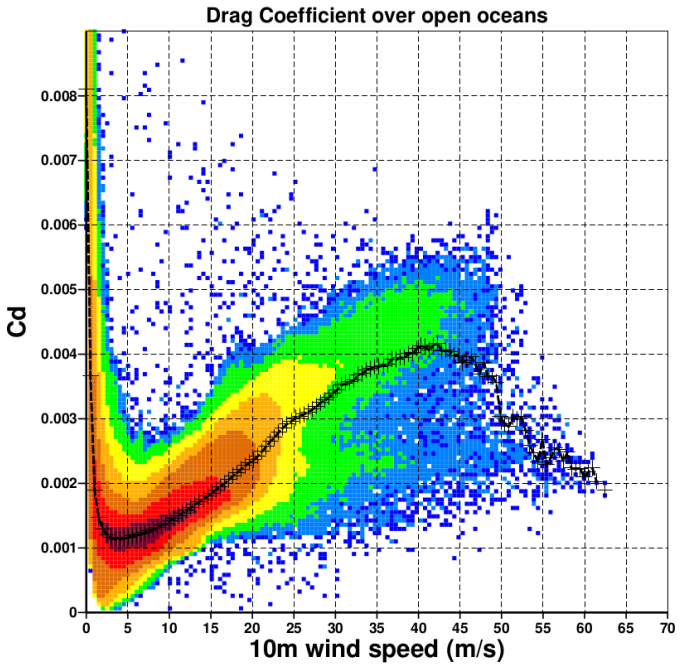

(a) C_{d} (CY46R1)

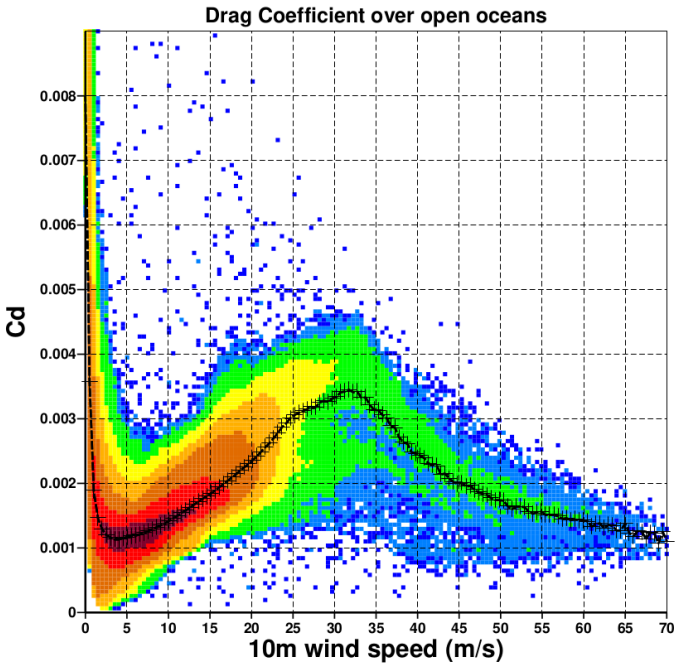

(b) C_{d} (CY47R1)

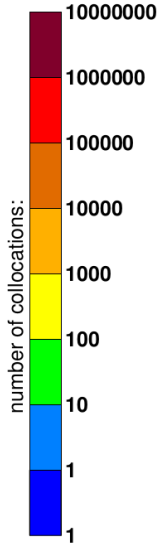

TCo1999 10-day forecast

Tropical cyclone max wind - min pressure relationship

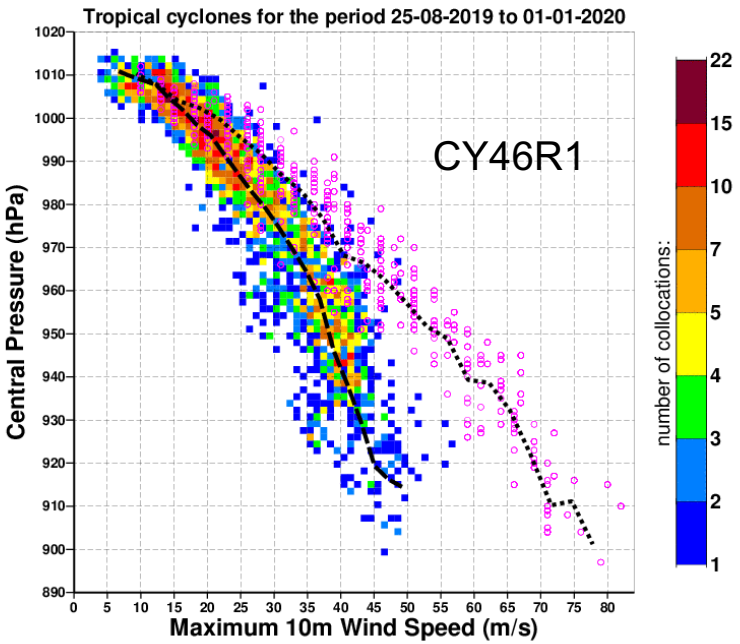

Colour shading and dashed line: TCo1279 forecasts (h9s0), all forecasts intialised from 0 UTC.
Pink symbols and dotted line: Best Track data.

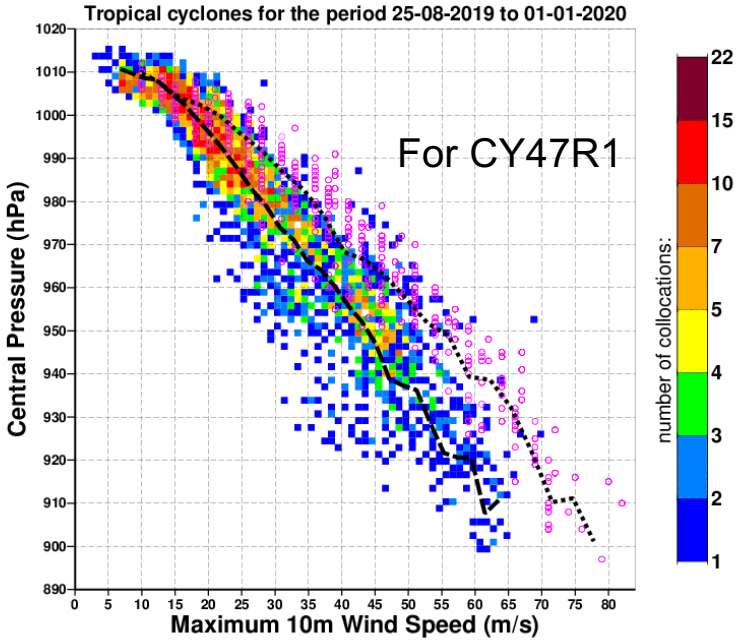

Colour shading and dashed line: TCo1279 forecasts (h9s3), all forecasts intialised from 0 UTC.
Pink symbols and dotted line: Best Track data.

Tco1279 forecasts from 0 UTC for period 25-08-2019 to 01-01-2020 (coloured shading and dotted line).
Reported values (pink symbols and dotted line) for tropical cyclones:
Ambali, Belna, Bualoi, Calvinia, Dorian, Faxai, Fengshen, Hagibis, Halong, Humberto, Kammuri, Kyarr, Lingling, Lorenzo, Maha, Matmo, Nakri, Phanfone, Sarai, Sebastien

Six-component MODIS albedo

- Represent dependence of direct solar beam albedo on zenith angle
- Updated wavelength dependence including snow albedo

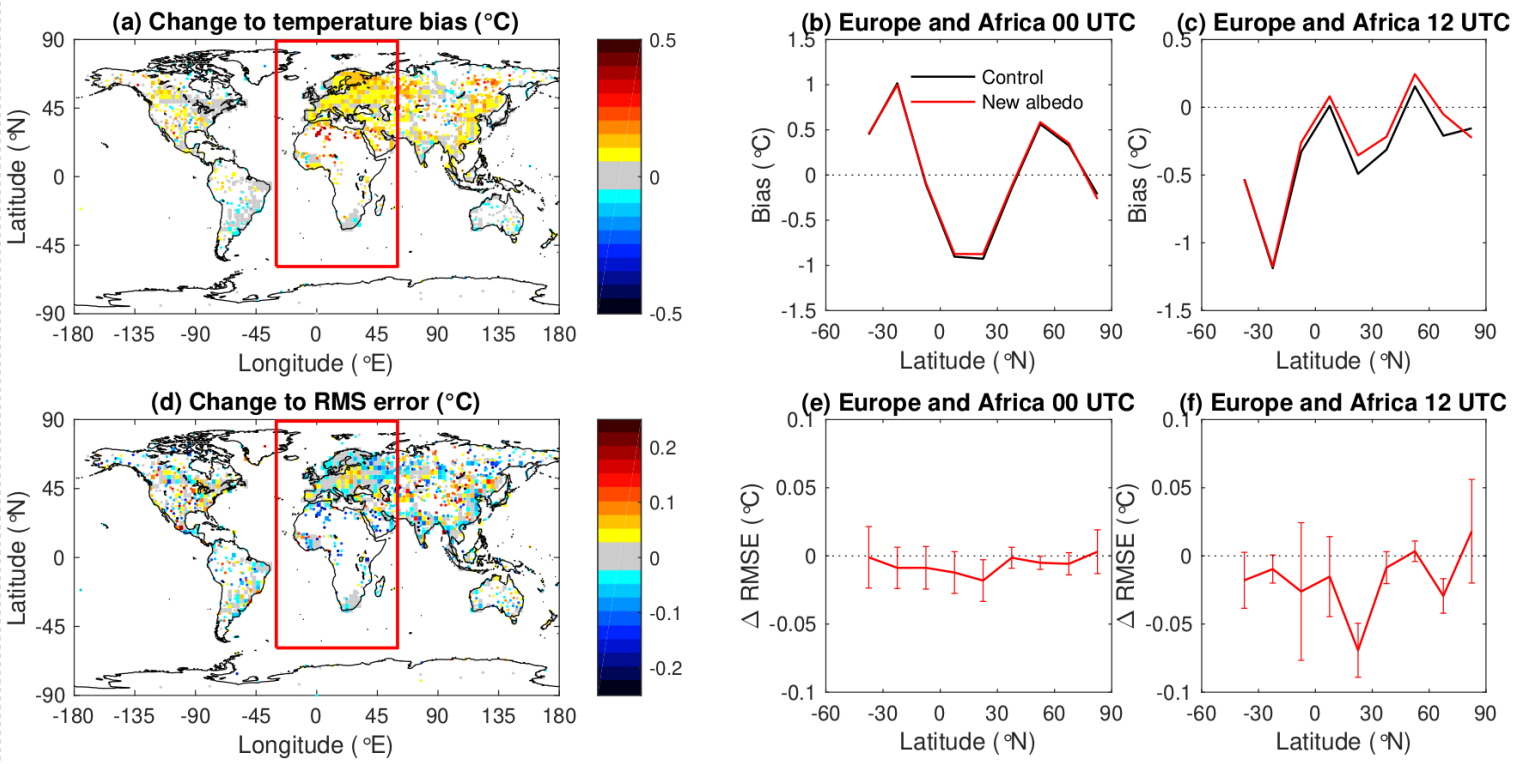

Revised convective inhibition diagnostic (CIN)

46r1

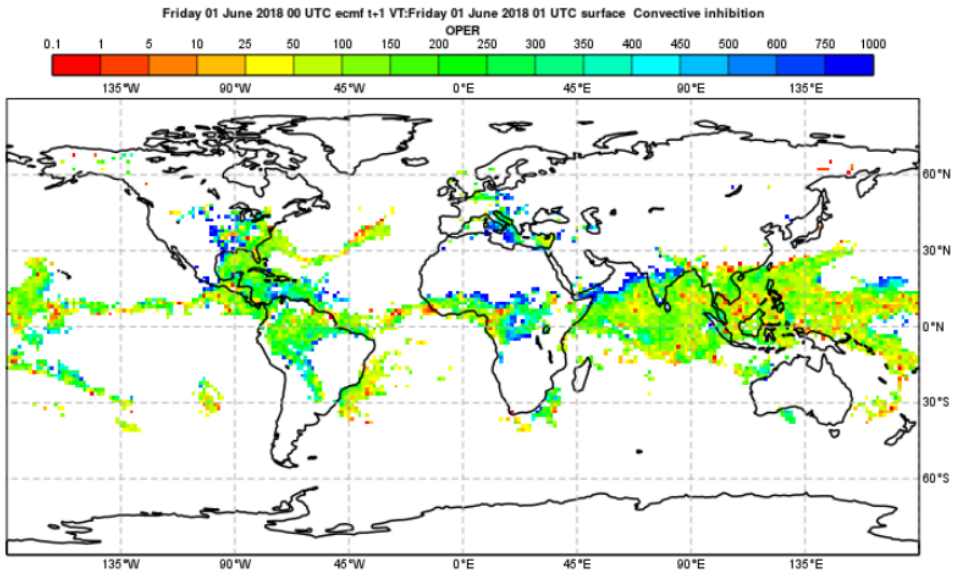

47r1

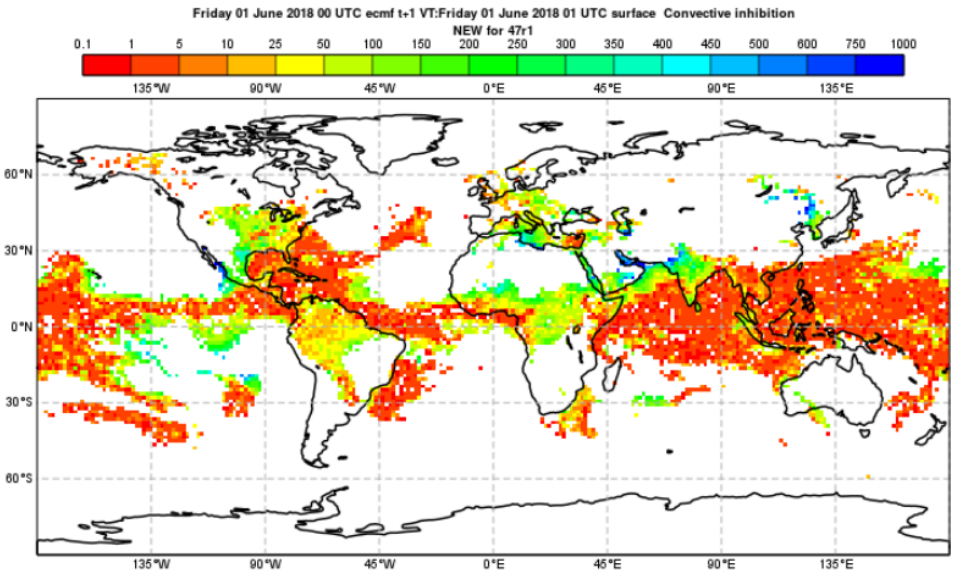

- CIN has been revised to use virtual potential temperature instead of equivalent potential temperature
- Considerable reduction in average CIN values

Medium-range ensemble score changes

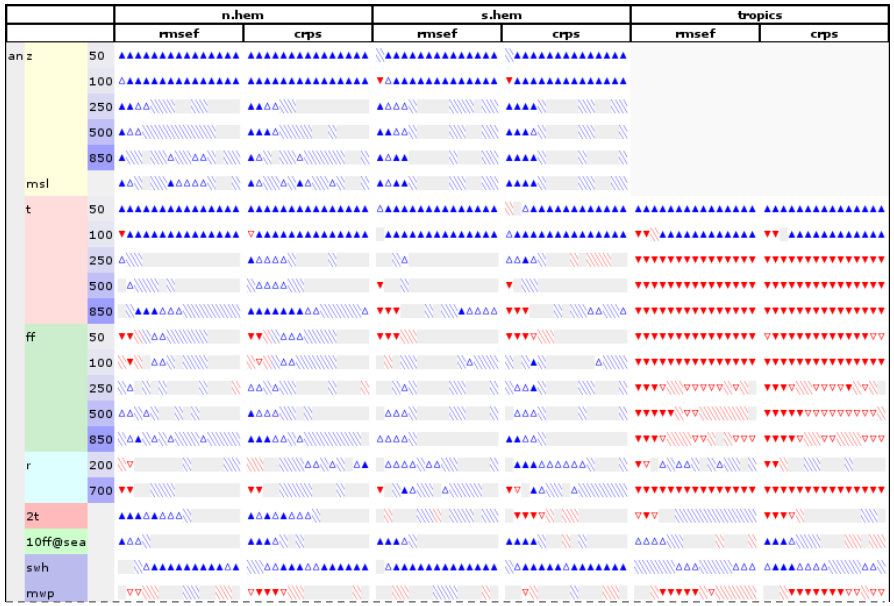

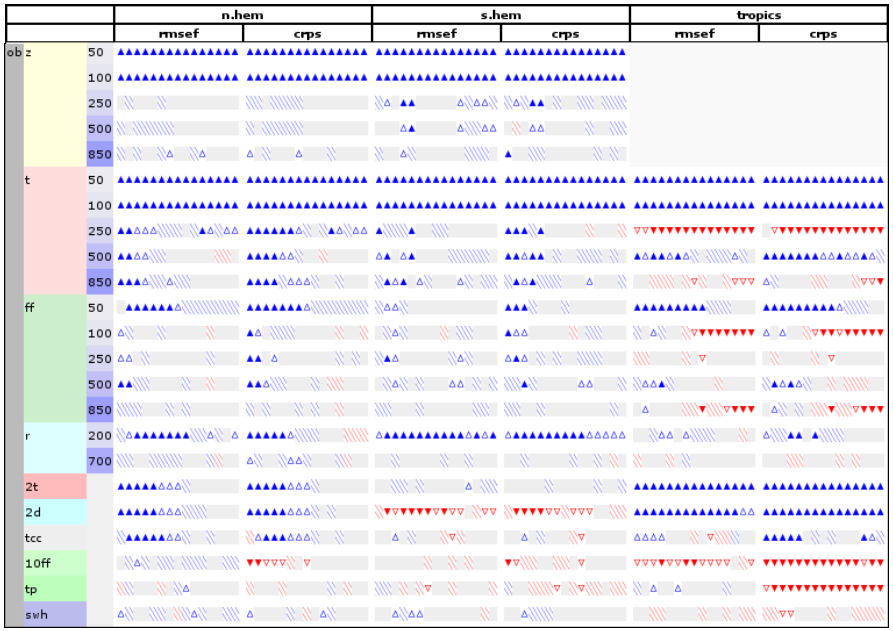

HRES score changes versus own analysis and observations

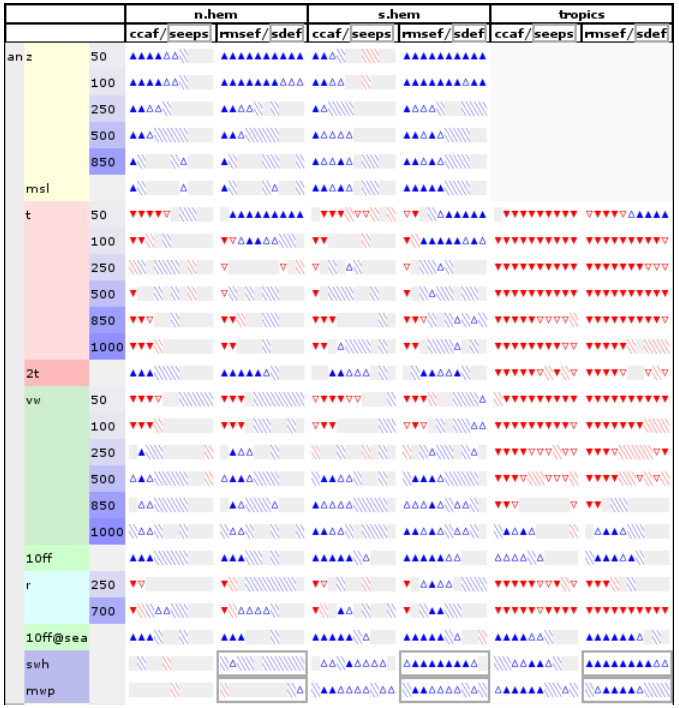

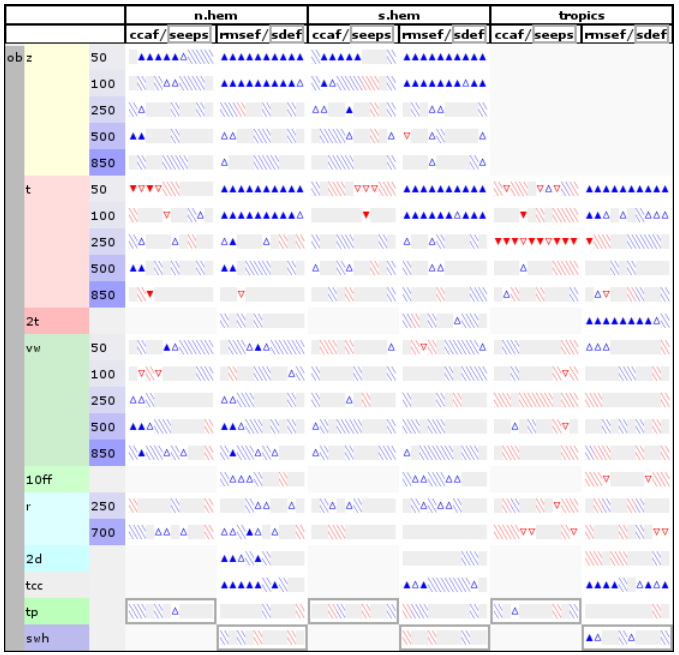

TC track error in HRES

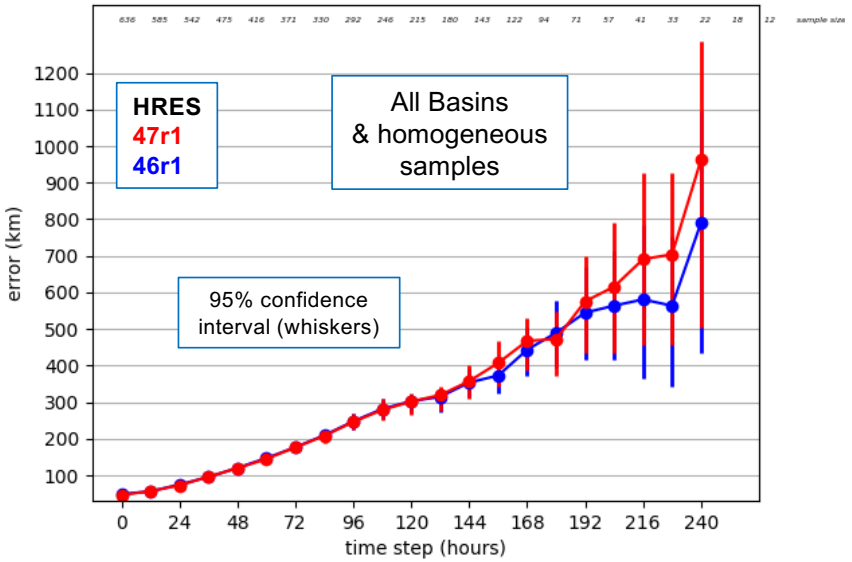

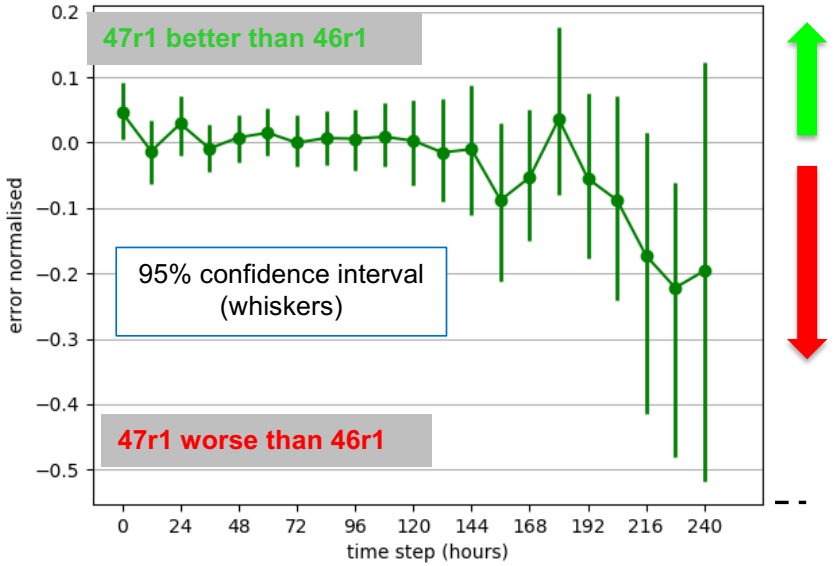

TC intensity error in HRES

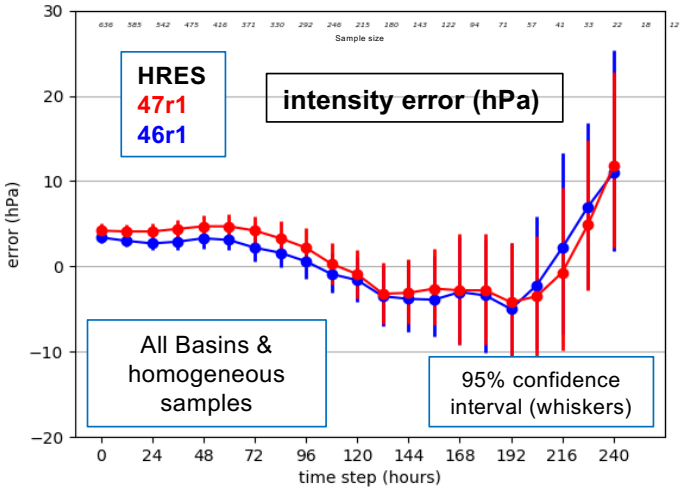

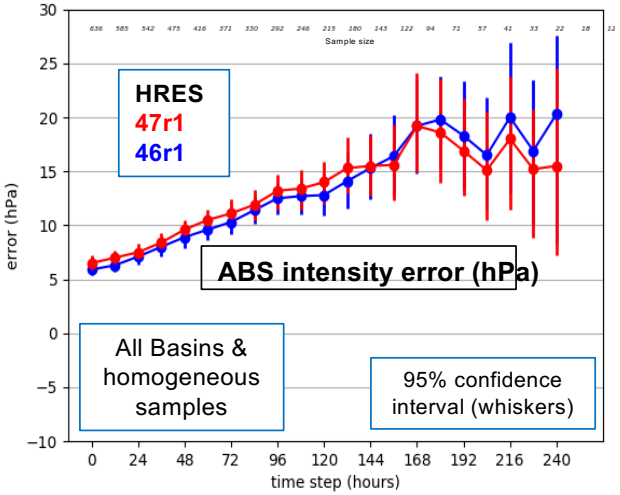

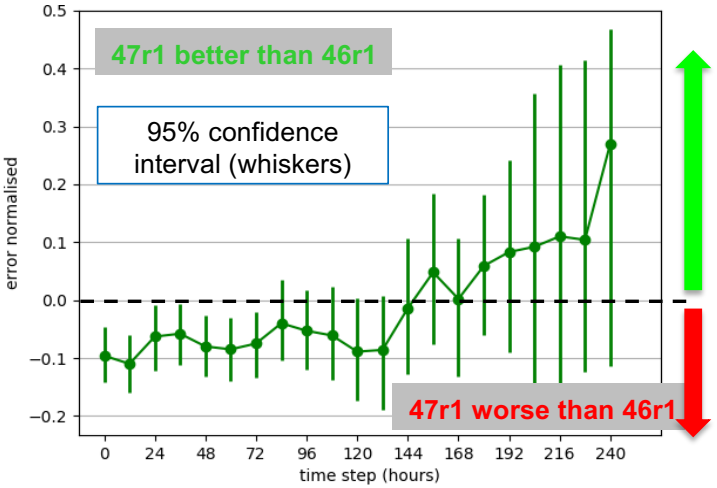

TC maximum wind error in HRES

Mean error

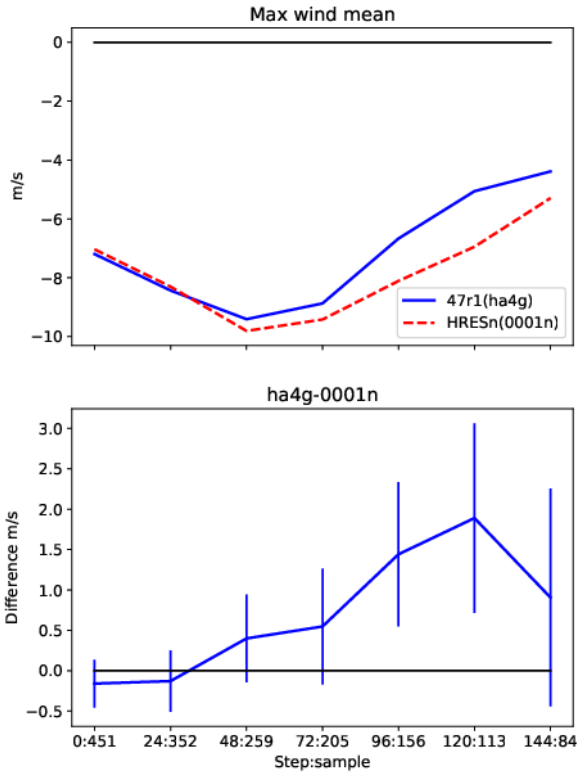

Mean absolute error

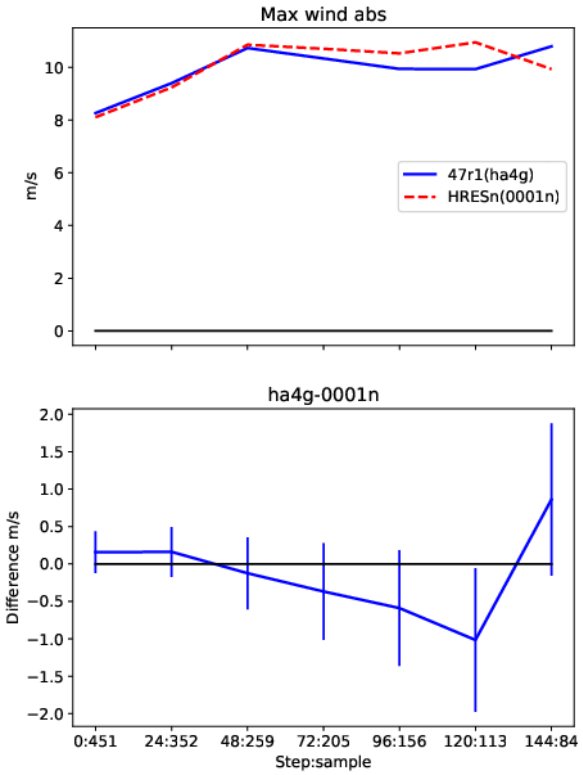

Wind pressure relation (based on all lead times in plots to the left)

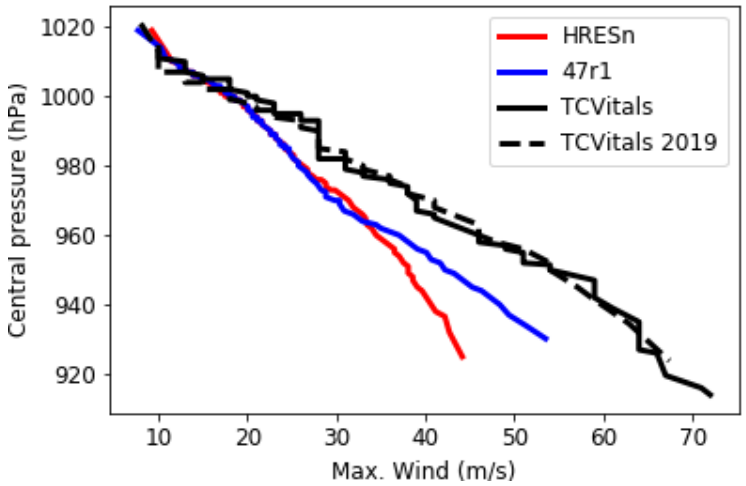

Extended-range impact on scores and MJO

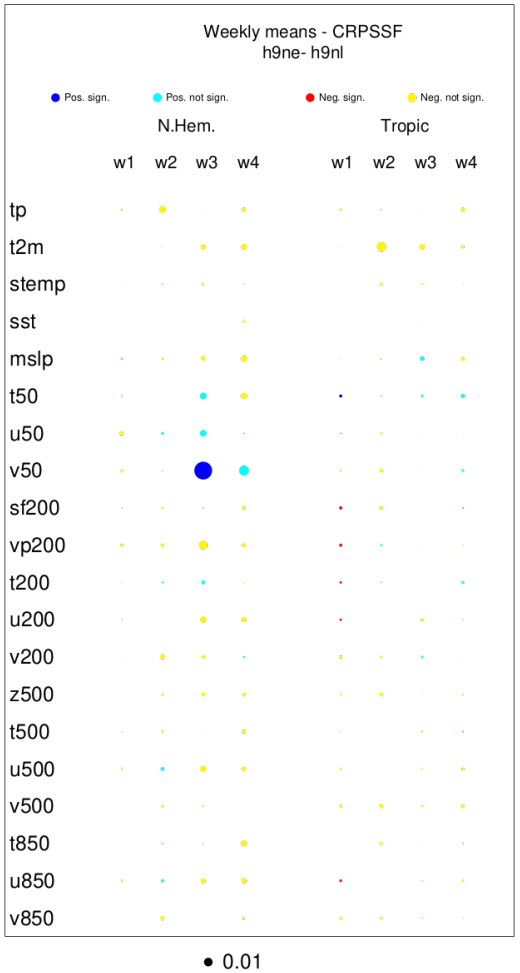

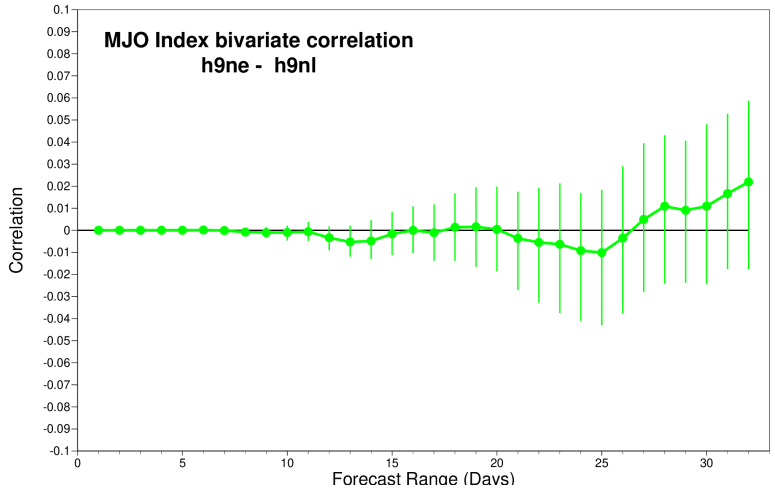

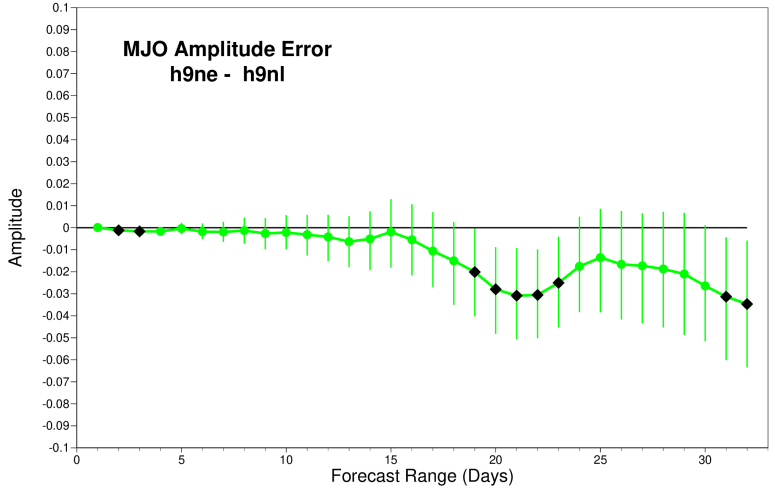

Next steps

- Implementation planned for June 30th
- Further webinars are planned in May (27th at 8:30 UTC; 28th at 14:30 UTC) with a focus on verification, technical access to the test data, and new parameters and products.
- Please do 'watch' the cycle 47r1 implementation wiki page to keep in touch with the latest news
  - https://confluence.ecmwf.int/display/FCST/Implementation+of+IFS+Cycle+47r1

ECMWF